J. Membrane Biol. 171, 35–46 (1999)

The Journal of
Membrane
Biology

An ATP-Sensitive K^+ Current that Regulates Progression Through Early G1 Phase of the Cell Cycle in MCF-7 Human Breast Cancer Cells

E. Klimatcheva*, **W.F. Wonderlin**

Department of Pharmacology and Toxicology, West Virginia University, Morgantown, WV 26505, USA

Received: 22 January 1999/Revised: 11 May 1999

Abstract. Whole-cell recordings were used to identify in MCF-7 human breast cancer cells the ion current(s) required for progression through G1 phase of the cell cycle. Macroscopic current-voltage curves were fitted by the sum of three currents, including linear hyperpolarized, linear depolarized and outwardly rectifying currents. Both linear currents, but not the outwardly rectifying current, were increased by 1 μM intracellular Ca^{2+} and blocked by 2 mM intracellular ATP. When tested at concentrations previously shown to inhibit proliferation by 50%, linogliride, glibenclamide and quinidine inhibited the linear hyperpolarized current, and quinidine and linogliride inhibited the linear depolarized current; none of these agents affected the outwardly rectifying current. In contrast, tetraethylammonium completely inhibited the outwardly rectifying current, but did not inhibit either linear current. Changing the bath solution to symmetric K^+ shifted the reversal potential of the linear hyperpolarized current from near the K^+ equilibrium potential (−84 mV) to −4 mV. Arrest of the cell cycle in early G1 by quinidine was associated with significantly smaller linear hyperpolarized currents, without a change in the linear depolarized or outwardly rectifying currents, but this reduction was not observed with arrest by lovastatin at a site ≈6 hr later in G1. The linear hyperpolarized current was significantly larger in *ras*-transformed than in untransformed cells. We conclude that the linear hyperpolarized current is an ATP-sensitive K^+ current required for progression of MCF-7 cells through G1 phase.

Key words: ATP-sensitive K channel — G1 phase — MCF-7 — Proliferation — Breast cancer

* *Present address:* University of Rochester, Cancer Center, Rm 1-3101, 575 Elmwood Ave., Rochester, NY 14642, USA

Correspondence to: W.F. Wonderlin

Introduction

There is substantial evidence that K^+ currents through K channels in the plasma membrane are required for proliferating cells to pass through the G1 phase of the cell cycle (reviewed in Wonderlin & Strobl, 1996). This requirement might, in fact, represent a checkpoint in G1 phase at which communication must occur between K channels in the plasma membrane and the cytosolic signaling pathways that regulate the cell cycle. Changes in membrane potential or cell volume produced by K^+ currents might stimulate or suppress specific cell cycle regulatory signals, and in a reciprocal manner, the activation of K channels might be controlled by signaling pathways that coordinate activation of the channels with other cell cycle regulatory signals. It appears that no single type of K channel ubiquitously regulates the cell cycle, and putative regulatory roles have been proposed for diverse types of K channels, including voltage-gated, Ca-activated and ATP-sensitive K channels (K_{ATP}) (reviewed in Wonderlin & Strobl, 1996). This diversity, in particular, challenges our ability to model communication between K channels and cell cycle regulatory signals during progression through G1 phase. Although K^+ currents arising from many types of K channels could stimulate regulatory pathways in an analogous manner, it is far more difficult to envision how cell cycle signaling pathways might regulate K channels as diverse as voltage-gated and ligand-gated K channels, channels whose gating is controlled by fundamentally different processes. Clearer insight into the communication between K channels and cell cycle regulatory signals can only be gained by a more rigorous identification of the K^+ currents that regulate progression through G1 phase and a more detailed characterization of how the activity of these K^+ currents can be regulated.

The activity of voltage-gated Kv1.3 channels has been demonstrated unambiguously to be required for the

mitogen-stimulated entry of lymphocytes into G1 phase (Price, Lee & Deutsch, 1989; Freedman, Price & Deutsch, 1992; Lin et al., 1993), but regulatory roles for other types of K channels are much less conclusively established. ATP-sensitive K channels (K_{ATP}) have been proposed by several investigators as putative regulators of passage through G1 phase, and a regulatory role for this class of K channel is particularly intriguing given their sensitivity to many potential regulatory signals (Edwards & Weston, 1993; Gopalakrishnan, Janis & Triggle, 1993; Ashcroft & Gribble, 1998; Shyng & Nichols, 1998; Baukrowitz et al., 1998). We previously reported that inhibitors of ATP-sensitive K channels, but not inhibitors of most voltage- and Ca-activated K channels, arrest MCF-7 human breast cancer cells in early G1 phase (Woodfork, Wonderlin & Strobl, 1995), and this arrest is associated with decreased expression of *c-myc* mRNA, a regulatory signal essential for passage through early G1 (Melkoumian, Wang & Strobl, 1997). Furthermore, MCF-7 cells hyperpolarize during passage through G1 and entry into S phase, and this hyperpolarization is associated with an increase in the relative permeability to K^+ (Wonderlin, Woodfork & Strobl, 1995). The arrest of MCF-7 cells in G1 phase by quinidine, a nonselective K channel antagonist, can be surmounted by cotreatment with the K^+ ionophore valinomycin (Wang et al., 1998), which indicates that the arrest by quinidine can be accounted for simply by it preventing an increase in the relative permeability to K^+. Collectively, these observations support a key role for K_{ATP} currents in regulating passage through G1 phase, but the presence of a K_{ATP} current in MCF-7 cells has not been established. In the present study we have focused on identifying a K^+ current in MCF-7 cells which can unify the observations described above, and we report that MCF-7 cells do, indeed, express a K_{ATP} current whose activation is required for progression through G1 phase.

Materials and Methods

Cell Culture

MCF-7 cells were grown in Dulbecco's Modified Eagle's Medium (DMEM) supplemented with 10% heat-inactivated fetal bovine serum, 0.04 mg/ml gentamicine and 2 mM glutamine, at 37°C in a humidified 5% CO_2–95% air incubator. Cells were passaged weekly at a ratio of 1:5. Passages 38–55 were used in this study. Cells for patch-clamp experiments were harvested with 0.02% trypsin and plated onto 5 mm square glass coverslips in 35 mm dishes at a density of 3.4×10^5 cells/dish 24 hr prior to recording.

Solutions and Chemicals

The standard bath solution for patch-clamp experiments was Hanks Buffered Salt Solution (HBSS) of the following composition (mM): NaCl (136), KCl (5.37), $CaCl_2$ (1.8), $MgCl_2$ (0.812), $NaHCO_3$ (4.17), Na-HEPES (15), glutamine (2), glucose (1 g/l), with the pH adjusted with HCl to 7.2. In some experiments the K^+ concentration was increased by equimolar replacement of NaCl with KCl, and the control NaCl concentration was increased to 144.63 mM. In other experiments, intracellular KCl was replaced with equimolar K-Gluconate. All recordings were made with the cells superfused in a small (40 μl) recording chamber.

Patch pipettes were filled with a standard intracellular buffer of the following composition (mM): KCl (150), $MgCl_2$ (1.0), H-HEPES (10), EGTA (0.5), glucose (10) with the pH adjusted to 7.4 with KOH. The composition of the Ca^{2+}/EGTA buffers was the same as used by Wegman, Young & Cook (1991) to study Ca-dependent K channels in MCF-7 cells: 0.193 μM free Ca^{2+} (1.92 mM EGTA and 0.97 mM $CaCl_2$); 0.5 μM free Ca^{2+} (1.93 mM EGTA and 1.53 mM $CaCl_2$); 1 μM free Ca^{2+} (1.73 mM EGTA and 1.53 mM $CaCl_2$). In all experiments the pH was adjusted to 7.4 with KOH. Unless otherwise noted, 10 mM Na-UDP and 100 μM Mg-ATP were added to the pipette solution to prevent "rundown" of K_{ATP} currents and 0.193 μM Ca^{2+} was added to facilitate seal formation. The osmolality of the bath and pipette solutions was adjusted to 330 ± 5 mOsm by addition of glucose.

Quinidine, tetraethylammonium (TEA), glibenclamide and 9-anthracene carboxylic acid (9-AC) were purchased from Sigma (St. Louis, MO). Linogliride was a gift from the R.W. Johnson Pharmaceutical Research Institute (Spring House, PA). Quinidine, TEA and linogliride were prepared as 10 mM stocks in distilled water; glibenclamide and 9-AC were prepared as a 50 mM stock solution in dimethylsulfoxide (DMSO). All stock solutions were made fresh daily and diluted into HBSS. Lovastatin was obtained from A.W. Alberts (Merck, Sharp & Dohme Research Pharmaceuticals, Rahway, NJ). Lovastatin was converted from its inactive lactone prodrug form to its active dihydroxy open acid form by first dissolving 5.9 mg of prodrug in 118 μl of 95% ethanol, then adding 92 μl of 1N NaOH and incubating for 2 hr at 50°C. The pH of the solution was adjusted to 7.2 with 1N HCl, and the volume was increased to 1.5 ml (10 mM) by the addition of water. The stock solution was stored at −20°C.

Electrophysiology

The whole-cell recording configuration of the patch-clamp technique was used to study membrane currents in MCF-7 cells. The ruptured-patch method was used to control the intracellular milieu and to allow us to test the effects of intracellular ATP and Ca^{2+} on membrane currents. All recordings were performed at room temperature (22–24°C). Pipettes were pulled from borosilicate glass capillaries (World Precision Instruments, Sarasota, Florida; w/fil., 1.5 mm o.d.), coated with Sylgard to within 0.2 mm of the tip and fire polished on a Narashige microforge.

Membrane currents were recorded using an Axopatch-1B amplifier. The currents were filtered and digitized at 5 kHz and analyzed using software written by W.F.W. Current-voltage relations were determined by measuring the membrane current at a series of stepped command potentials between −80 and +40 mV (10 mV increments) with a holding potential between steps of −50 mV. The duration of each step was 800 msec, with an interval of 1 sec between steps, and the current amplitude was calculated as the average current during the last 50 msec of each voltage step. The size of MCF-7 cells was highly variable. To facilitate comparisons among cells, we converted the current amplitudes to current densities by dividing each current amplitude by the cell capacitance indicated by the capacity compensation adjustment. The pipette liquid junction potential calculated from the Henderson equation (Barry & Lynch, 1991) for our standard recording conditions (HBSS in the bath and the high-K solution in the pipette) was −4 mV, which was subtracted from the command voltages prior to display and analysis of the data.

Cell Synchronization

The HMB-CoA reductase inhibitor lovastatin and the K channel blocker quinidine were used to arrest cells in G1 phase. Cells were plated at a density of 7×10^4 cells/well into 6-well plates containing 10% DMEM. The medium was removed 40 hr after plating and replaced with medium containing 30 μM lovastatin or 90 μM quinidine. Membrane currents were measured 30 hr after addition of the drugs.

Curve Fitting/Data Analysis

Each whole-cell *I/V* curve was fitted by the sum of three currents, including a linear hyperpolarized (I_{lh}), a linear depolarized (I_{ld}) and a voltage-dependent, outwardly rectifying (I_{or}) current, as indicated in the following equation:

$$I = G_{LH}(V_C - E_{LH}) + G_{LD}(V_C - E_{LD}) + \frac{G_{OR}(V_C - E_{OR})}{1 + \exp\left(-\frac{V_C - V_{0.5}}{k}\right)} \qquad (1)$$

where I is the total membrane current density; V_C is the step command potential; E_{LH}, E_{LD} and E_{OR} are the reversal potentials for the linear hyperpolarized, linear depolarized and voltage-dependent components, respectively; and G_{LH}, G_{LD}, and G_{OR} are the conductance densities for the three components. $V_{0.5}$ is the membrane potential for half-maximal activation and k is the slope parameter for the voltage-dependent current, I_{or}.

The relative sizes of the three components in each *I/V* curve were estimated by adjusting the parameters G_{LH}, G_{LD}, and G_{OR}, using the Simplex algorithm, to optimize a least-squares fit to the *I/V* curve. All other parameters were held constant at the following values. E_{LH}, E_{LD} and E_{OR} were assumed to be the Nernst potential for K^+ (−84 mV), the reversal potential of a TEA-sensitive linear current (−4 mV), and the median reversal potential (−52.5 mV) calculated for six outwardly rectifying tail-currents, respectively. $V_{0.5}$ and k were estimated by fitting five *I/V* curves recorded with 2 mM ATP in the pipette by the sum of an outwardly rectifying component and a small, linear leak component. These parameters were estimated to be +29.2 mV and 15.2 mV, respectively.

For each blocking drug tested, the functional block, F_B, was calculated as $(G_{control} - G_{drug})/G_{control}$. The mean fractional block was calculated at each concentration from experiments in which the conductance density of the component was $\geq 1 \times 10^{-4}$ nS/pF, and the component constituted at least 10% of the cell's total conductance density. The exclusion of smaller components helped reduce the variability in the estimates of the means. These concentration response curves were fitted by:

$$F_B = \frac{B_{max}}{1 + \left(\frac{K_i}{D}\right)^h} \qquad (2)$$

where B_{max} is the maximum fractional block, K_i is the concentration at which the block was half maximal, D is the concentration of drug and h is the Hill coefficient. The means were fitted using a nonlinear least squares method (JMP Statistical software, SAS Institute), with each mean weighted by the reciprocal of the standard error of the mean (SEM).

Statistical analysis was performed using JMP software. Student's *t*-test for multiple comparisons modified by the Tukey-Kramer HSD method was used to compare treatment means with control means, and one-sided *t*-tests were used to test the significance of drug block with $p < 0.05/n$, where n is the number of tests, considered to be significant. Means are plotted ±SEM.

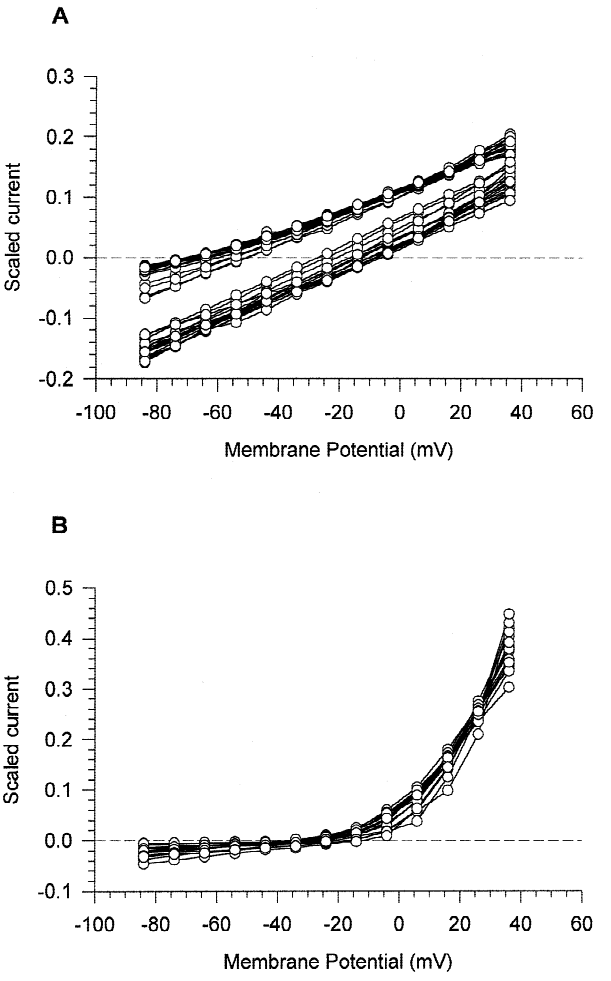

Fig. 1. Current-voltage relations in unsynchronized MCF-7 cells. Data were scaled so that the area under all *I/V* curves was equal to one (*A*) Cells with predominantly linear *I/V* relations ($n = 37$). (*B*) Cells with strongly outwardly rectifying *I/V* relations ($n = 17$).

Results

Current-Voltage Relations of Exponentially Growing MCF-7 Cells

The *I/V* relations for 54 randomly selected, unsynchronized, exponentially growing MCF-7 cells are shown in Fig. 1. These *I/V* curves have been scaled to the same area by dividing each *I/V* curve by the sum of the absolute values of the data points for the curve, thereby eliminating differences among *I/V* curves due to size. With this scaling, the *I/V* curves could be unambiguously divided into three clusters, distinguished by their linearity and reversal potential. The predominantly linear *I/V*

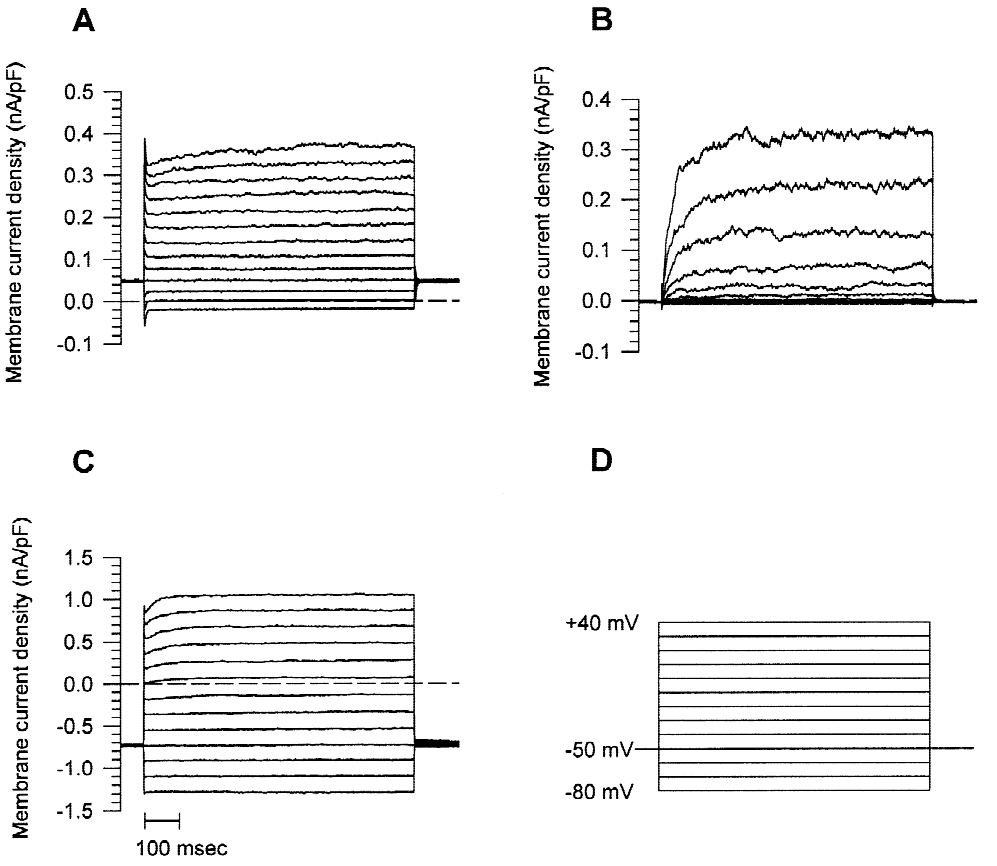

Fig. 2. Macroscopic membrane currents in unsynchronized MCF-7 cells. The currents were elicited by voltage steps from a holding potential of −50 mV to test potentials between −80 and +40 mV, in 10 mV increments (*see* Materials and Methods). (*A*) Linear hyperpolarized current (I_{lh}), (*B*) outwardly rectifying current (L_{or}), (*C*) linear depolarized current (I_{ld}) (*D*) Voltage-step protocol. Each set of whole-cell currents shown was recorded from a different cell.

curves (Fig. 1*A*) clustered into two groups based on their reversal potential, including linear hyperpolarized (reversal potentials ranging from −49 to −73 mV) and linear depolarized (reversal potentials ranging from −6 to −27 mV) curves. The third cluster included *I/V* curves displaying strong outward rectification (Fig. 1*B*). This clustering of the *I/V* curves suggested the presence of at least three macroscopic currents, including linear hyperpolarized (I_{lh}), linear depolarized (I_{ld}) and outwardly rectifying (I_{or}) currents.

Although the *I/V* curves frequently included a mixture of I_{lh}, I_{ld} and I_{or}, we did record whole-cell currents in which a single type of current predominated, and these recordings highlight important differences among the currents, as shown in Fig. 2. I_{or} could be easily distinguished from I_{lh} and I_{ld} as it was evoked only at membrane potentials more positive than ≈−10 mV, and it exhibited a delayed activation (Fig. 2*B*). I_{or} did not inactivate during the voltage step. I_{lh} (Fig. 2*A*) and I_{ld} (Fig. 2*C*) did not exhibit any voltage- or time-dependent properties. The small delay in activation at positive potentials evident in the recordings shown in Figs. 2*A* and 2*C* is due to a small contribution by I_{or}.

The absence of selective antagonists for each of these currents prevented us from using a pharmacological approach to separate the currents effectively. As an alternative, we used a curve-fitting procedure (described in Materials and Methods) to estimate the contribution of I_{lh}, I_{ld} and I_{or} to each *I/V* curve, and this enabled us to test the sensitivity of each of the three currents to experimental manipulations. We do recognize, however, that each of these currents might represent the sum of currents produced by more than one type of ion channel. With this caveat in mind, the goal of the experiments described below was to determine which of the three macroscopic currents, I_{lh}, I_{ld} and I_{or}, was most likely to include a current required for the progression of MCF-7 cells through G1 phase of the cell cycle.

Effects of Intracellular Ca^{2+}

A small conductance (23 pS), Ca^{2+}-activated K^+ channel has been described in MCF-7 cells (Wegman et al., 1991). We have observed that application of the Ca^{2+} ionophore ionomycin to MCF-7 cells elicited a rapid,

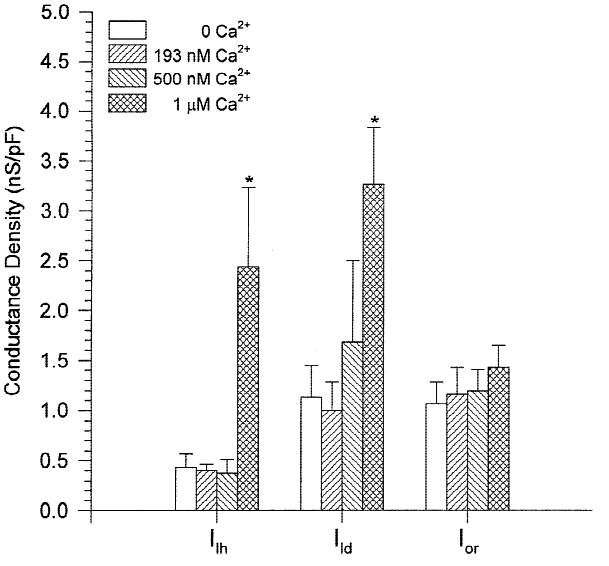

Fig. 3. Effect of intracellular Ca^{2+} on whole-cell currents. Currents were recorded either without Ca^{2+} in the pipette (control, $n = 40$) or Ca^{2+} concentrations of 193 nM ($n = 38$), 500 nM ($n = 31$) and 1 μM ($n = 21$). Groups that were significantly different from control values are marked by an asterisk.

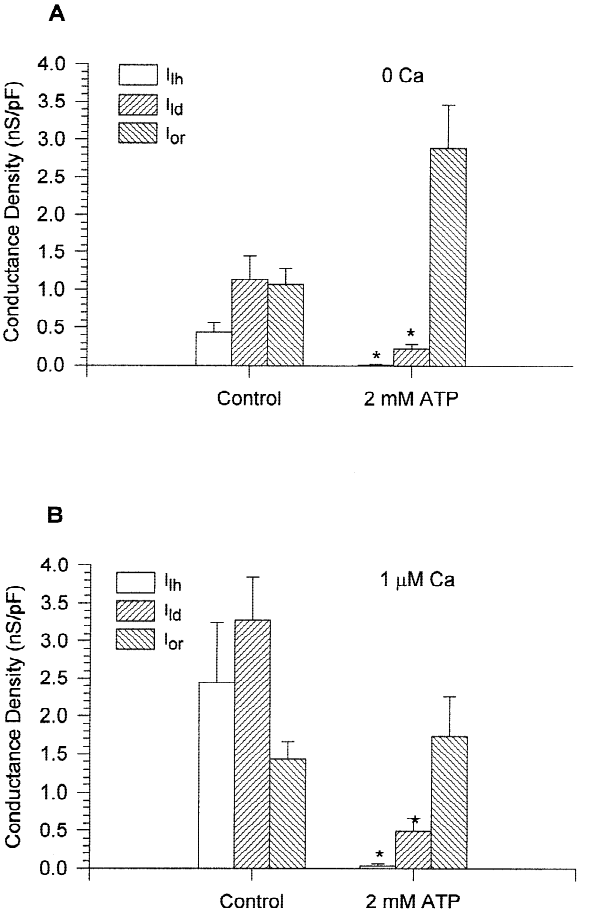

Fig. 4. Effects of intracellular ATP on whole-cell currents. (*A*) Whole-cell currents were recorded with 0 Ca^{2+} (control; $n = 40$) or 2 mM ATP ($n = 6$). (*B*) currents in the control group were recorded with 1 μM Ca^{2+} in the pipette ($n = 21$) and compared with currents recorded with 2 mM intracellular ATP ($n = 6$). Significant decreases in conductance densities, compared to control values, are marked by asterisks.

quinidine-sensitive hyperpolarization of the membrane potential (*our unpublished observations*), and, therefore, we predicted that a Ca^{2+}-dependent K^+ current would be present in the MCF-7 cells. We tested this prediction by adding 193 nM, 500 nM or 1 μM Ca^{2+} to the pipette solution. Only the highest Ca^{2+} concentration (1 μM) tested significantly increased any of the components, producing a 6-fold stimulation of I_{lh} and a 3-fold stimulation of I_{ld} (Fig. 3). I_{or} was not affected by Ca^{2+} at the concentrations tested. I_{lh} and I_{ld} were also present in the absence of Ca^{2+}, indicating either that activation of these currents was not entirely dependent on Ca or that a mixture of Ca-dependent and Ca-independent currents contributed to I_{lh} and I_{ld}.

Effects of Intracellular ATP

We tested the hypothesis that ATP-sensitive currents are present in MCF-7 cells by determining the sensitivity of whole-cell currents to the addition of 2 mM ATP to the pipette solution. Both I_{lh} and I_{ld} were significantly inhibited by 2 mM ATP added to a pipette solution containing either 0 or 1 μM Ca^{2+} (Fig. 4). I_{lh} was nearly completely inhibited (>98%) with either 0 or 1 μM Ca^{2+} in the pipette solution, indicating that all of the current(s) contributing to I_{lh} were sensitive to ATP, and this ruled out any contribution by an ATP-insensitive, Ca^{2+}-activated current to I_{lh}. On the other hand, I_{ld} was blocked by 82% with 0 Ca^{2+} in the pipette and by 85% with 1 μM Ca^{2+} in the pipette, indicating that a small, ATP-independent current also contributed to this component. I_{or} was not inhibited by ATP.

Effects of K Channel Blockers

The current whose activation is required for progression through early G1 phase should be blocked by glibenclamide, linogliride and quinidine, drugs which inhibited proliferation and progression through G1 phase, but not by TEA, which inhibited proliferation without arresting the cell cycle (Woodfork et al., 1995). We first tested the effects of each drug on the macroscopic currents at concentrations most relevant to inhibiting proliferation (Fig. 5). Drugs were added to the bath solution since they all inhibited the proliferation of MCF-7 cells when added to the culture medium. Quinidine (25 μM), linogliride (770 μM) and glibenclamide (50 μM) were tested at their IC_{50} concentration for inhibiting the proliferation of MCF-7

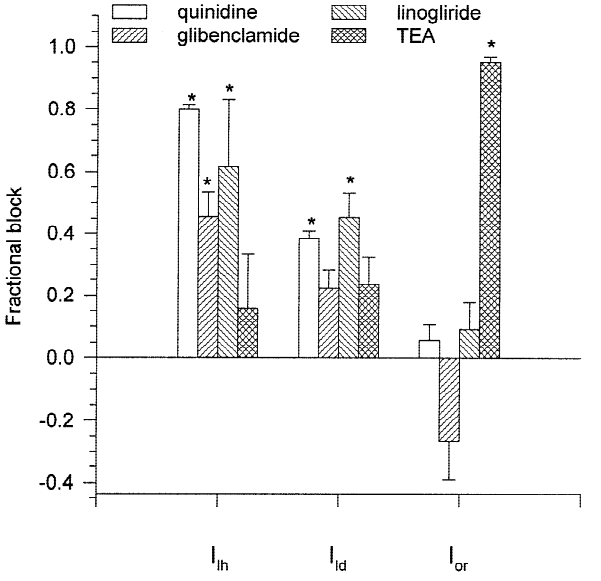

Fig. 5. Effects of K channel antagonists on whole-cell currents. The fractional block of I_{lh}, I_{ld} and I_{or} is shown for each drug (n = 4–15) cells. Quinidine, glibenclamide, linogliride and TEA were tested at concentrations of 25 μM, 50 μM, 770 μM and 10 mM, respectively. Statistically significant block is marked by an asterisk.

cells, and TEA was tested at 10 mM, its IC_{65} concentration for inhibiting proliferation (Woodfork et al., 1995). The three currents exhibited distinctly different patterns of sensitivity to the four antagonists. I_{lh} was reversibly blocked by quinidine, glibenclamide and linogliride, but not by TEA. I_{ld} was blocked by quinidine and linogliride, but not by TEA or glibenclamide. I_{or} was nearly completely blocked by TEA, but it was not inhibited by the other drugs. The blocking action of all of the drugs was completely reversible (*data not shown*). Of the three currents, only I_{lh} matched the pharmacological profile expected for the target of the drugs that arrest the cell cycle in G1 phase.

A more detailed examination of the dose-dependent inhibition of I_{lh}, I_{ld} and I_{or} is shown in Fig. 6. The dose-response data were fitted using Eq. 2, and the fitted curves are shown in Fig. 6 with the parameters for the fits given in the Table. The block of I_{lh} by quinidine was fitted well by a single-site blocking model, with saturating maximum block and a Hill coefficient not significantly different from 1. The variable block of I_{ld} and I_{or} by quinidine was not fitted. In contrast, glibenclamide and linogliride produced a steeply concentration-dependent block of I_{lh}, with Hill coefficients and B_{max} values for both drugs near 8 and 0.6, respectively. Glibenclamide and linogliride also inhibited I_{ld} with K_i values similar to those for inhibition of I_{lh}, but with lower values for B_{max} and the Hill coefficients (Table).

Ion Selectivity of I_{LH}, I_{LD} and I_{OR}

The equilibrium potentials for K^+, Na^+ and Cl^- calculated for extracellular HBSS and our standard pipette

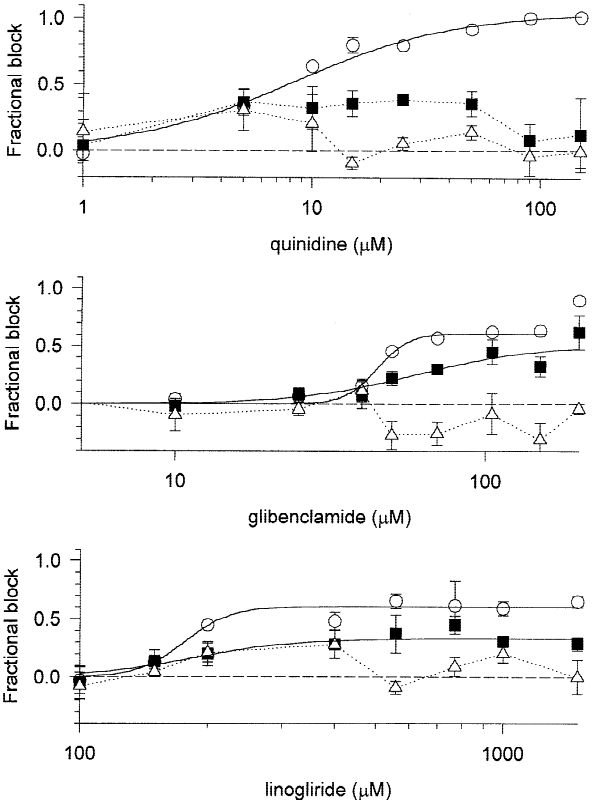

Fig. 6. Concentration-dependent inhibition of I_{lh}, I_{ld} and I_{or}. The upper, middle and lower panels show dose-response curves for quinidine, glibenclamide and linogliride, respectively. The data are plotted as the mean ± SEM of 3–7 experiments. SEM bars smaller than the symbols are not shown. I_{lh} is plotted as open circles, I_{ld} is plotted as filled boxes and I_{or} is plotted as open triangles. Least-squares fits of dose-response curves are plotted as solid lines, and the parameter values are given in the Table. For datasets that could not be fitted, the data points are connected by dotted lines. The data point for 200 μM glibenclamide was not included in the fit of I_{lh}.

Table. Best-fit parameters for concentration-dependent inhibition of I_{lh} and I_{ld}

	Component	K_i (μM)	B_{max}	h
Quinidine	I_{lh}	8.36	1.05	1.24
Glibenclamide	I_{lh}	44.82	0.61	8.67
	I_{ld}	61.12	0.52	2.26
Linogliride	I_{lh}	176.22	0.61	8.19
	I_{ld}	185.51	0.33	3.66

See Materials and Methods for a description of the curve-fitting procedure.

solution were −84, +69 and +0.9 mV, respectively. Clearly, the cluster of *I/V* curves associated with I_{lh} was closest to E_K (Fig. 1*A*). When I_{ld} was partially suppressed by 20 mM TEA, we observed *I/V* curves in some cells that indicated dominance by a current with a reversal potential very near E_K. An example is shown in Fig.

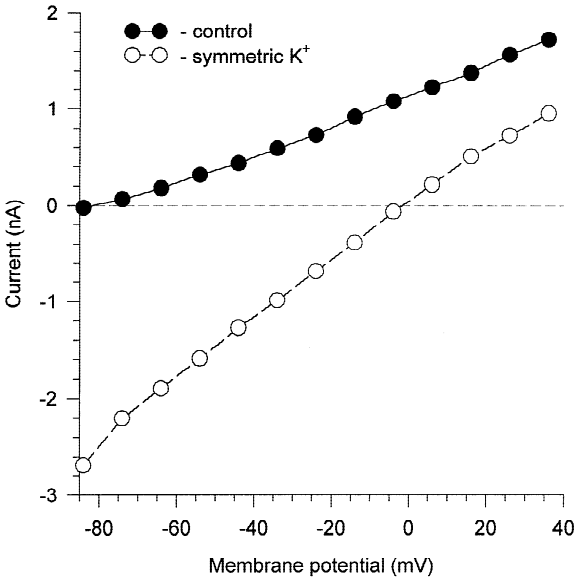

Fig. 7. I_{lh} is selective for K^+. I_{or} was eliminated and I_{ld} reduced by adding 20 mM TEA to the bath solution. Current/voltage relations are shown for a single cell recorded with a K^+ gradient (5.37 mM KCl in the bath, 150 mM KCl in the pipette, filled circles) and in symmetrical 150 mM K^+ (open circles).

7, in which *I/V* curves are shown for a cell recorded first in HBSS and then in symmetric 150 mM KCl with TEA (20 mM) added to both solutions. The reversal potential of the *I/V* curve shifted from ~−85 to ~−4 mV when the HBSS solution was changed to symmetric K^+, which is very close to the shift predicted for a K^+-selective current. In symmetric K^+, the *I/V* relation also exhibited a slight inward rectification, as expected for a K_{ATP} current (Zhou, Tate & Palmer, 1994).

The ion selectivity of I_{ld} was more difficult to determine because we could not pharmacologically isolate it from I_{lh}. Our best estimate of the reversal potential of I_{ld} was obtained from recordings in which I_{or} was absent and I_{lh} was very small, in which case TEA blocked a current with a reversal potential near −4 mV, a reversal potential consistent with either a nonselective cation current or a chloride current. We tested several inhibitors of nonselective cation channels, including 50 μM flufenamic acid, 1 μM amiloride and 1 mM gadolinium chloride (*data not shown*). Among these agents, only the addition of gadolinium chloride to the pipette solution inhibited I_{ld}, decreasing the current by 41.0 ± 7% (n = 3) and shifting the reversal potential in the hyperpolarized direction by −22.0 ± 6 mV (n = 3). These observations support a tentative conclusion that I_{ld} probably includes a nonselective cation current.

To determine if a Cl^- current might also contribute to I_{ld}, we substituted the internal KCl with either equimolar K-Gluconate or K-Acetate, and 20 mM TEA was added to the bath. Both substitutions revealed a small, outwardly rectifying current (Fig. 8) which could

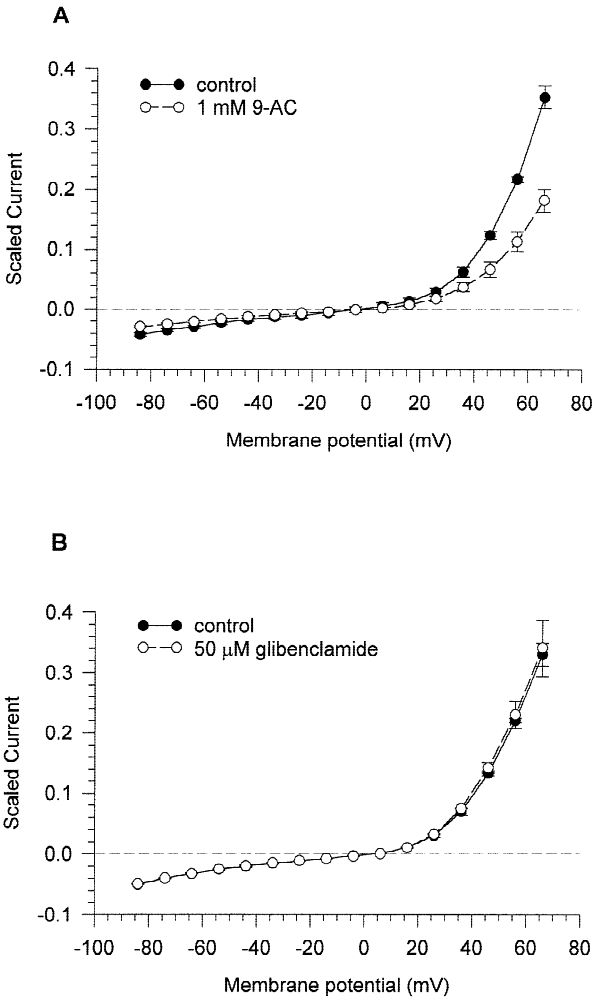

Fig. 8. Pharmacology of an outwardly rectifying Cl^- current. An outwardly rectifying Cl^- current was elicited by equimolar substitution of the 150 mM KCl in the pipette solution with KGlu, and I_{or} was blocked by adding 20 mM TEA to the HBSS. Currents were measured at step command potentials from −80 to +60 mV, with a holding potential of −50 mV, in 10 mV increment. For each pair of control and drug-exposed recordings from a single cell, the area under the control curve was scaled to an area of one, and the same scale factor was used to scale the drug-exposed data. The scaled data were averaged and are plotted as the mean ± SEM. (*A*) 1 mM 9-AC partially inhibited the current (n = 5). (*B*) 50 μM glibenclamide did not inhibit the rectifying current (n = 2).

be distinguished from I_{or} because: (i) it was observed only in the presence of a very steep Cl^- gradient, (ii) its reversal potential was more depolarized and it did not shift significantly in symmetric K^+ (*data not shown*), and (iii) the current was insensitive to 20 mM TEA. The reversal potential of the TEA-insensitive, outwardly rectifying current was very depolarized (0 to −20 mV) compared to the Cl^- equilibrium potential (−109 mV), perhaps due to the ability of the anions substituted for Cl^- to permeate the channels or the presence of a small background current with a more depolarized reversal poten-

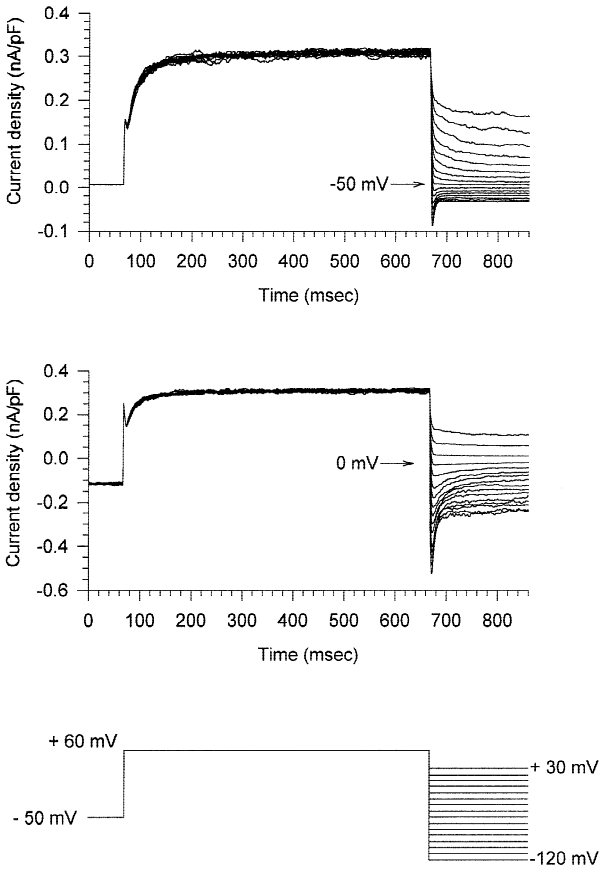

Fig. 9. Ion selectivity of the outwardly rectifying current. I_{lh} and I_{ld} were blocked by adding 2 mM ATP to the pipette solution. The cell was held at −50 mV, depolarized to +60 mV and then hyperpolarized to potentials from +30 to −120 mV (lower panel). The tail currents were recorded in either 5.37 mM $[K^+]_o$ (upper panel) or 150 mM $[K^+]_o$ (middle panel). The currents were not leak subtracted.

tial. The TEA-insensitive, outwardly rectifying current was blocked nearly 50% by bath application of 1 mM 9-anthracene carboxylic acid (9-AC), an agent that blocks Cl^- channels in epithelial cells and cardiac myocytes (Fig. 8*A*) (Welsh, 1984; Harvey, Clark & Hume, 1990). I_{lh}, I_{ld} and I_{or} were not affected by 9-AC (*data not shown*). Glibenclamide can inhibit myocardial and epithelial Cl^- channels at high concentrations (100 μM) (Sheppard & Welsh, 1992; Tominaga et al., 1995), but 50 μM glibenclamide, which inhibited the proliferation of MCF-7 cells by 50% (Woodfork et al., 1995) did not affect the TEA-insensitive, outwardly rectifying current (Fig. 8*B*).

The ion selectivity of I_{or} was investigated by examining the reversal potential of tail currents (Fig. 9). Cells were held at −50 mV, depolarized to +60 mV, and then stepped in 10 mV increments from +30 to −120 mV. I_{lh} and I_{ld} were blocked by 2 mM ATP added to the pipette solution. Tail currents recorded from cells bathed in HBSS (5.37 mM $[K^+]_o$) reversed at −52.5 ± 2.5 mV (n = 6), from which a P_K/P_{Na} permeability ratio of 12 was calculated from the GHK equation, indicating a selectivity of I_{or} for K^+ over Na^+. Based on this P_K/P_{Na} value, the reversal potential under symmetric conditions (150 mM $[K^+]$) was predicted to be 0 mV, and, as shown in Fig. 9 (middle traces), the tail currents recorded in symmetric 150 mM $[K^+]$ reversed at approximately 0 mV, close to the predicted value.

Current-Voltage Relations of Cells Arrested in Early G1

We previously reported that the membrane potentials of MCF-7 cells arrested in early G1 phase are depolarized relative to the membrane potentials of cells accumulated in S phase (Wonderlin et al., 1995), and we hypothesized that the difference in membrane potential results from the cells having a lower relative K permeability during early G1 phase than in S phase. If the lower relative permeability to K^+ is associated with a decreased activation of I_{lh}, then the average conductance density of I_{lh} should be lower in cells arrested in early G1 phase than in control, unsynchronized cells. We compared the currents recorded from cells arrested by either quinidine or lovastatin, an inhibitor of cholesterol biosynthesis; both of these drugs have been shown to arrest reversibly the cell cycle of MCF-7 cells in early G1 phase (Keyomarsi et al, 1991; Woodfork et al, 1995). Quinidine arrests the cell cycle of MCF-7 cells at a site approximately 12 hr after entry into G1, and the site of arrest by lovastatin is 5–6 hr after the site of arrest by quinidine (Wang et al., 1998).

Cells were treated with 30 μM lovastatin or 90 μM quinidine, concentrations previously shown to increase the percentage of cells in G0/G1 to 80–85% after 30 hr treatment. To minimize direct effects of the drugs on ion currents, the cells were washed in drug-free DMEM for 30 min prior to recording. The time allowed for washout was estimated from whole-cell recordings in which inhibition of linear currents by quinidine was fully reversed within 15 min after beginning washout of the drug (*see also* Fig. 3 in Wang et al., 1998). Quinidine and lovastatin increased the percentage of cells in G0/G1 by 21 ± 2% (n = 2) and 15 ± 2% (n = 2), respectively. Arrest of the cell cycle by lovastatin did not affect the conductance density of any of the three components of the *I/V* (n = 18), whereas arrest by quinidine significantly decreased the conductance density of I_{lh} by 96% relative to control (n = 13, Fig. 10). Arrest by quinidine did not affect the conductance densities of I_{ld} and I_{or}.

Overexpression of Ras-Oncogene Increases I_{LH}

MCF-7 cells transformed with the *ras* oncogene have a shorter G1 transit time than control, untransformed

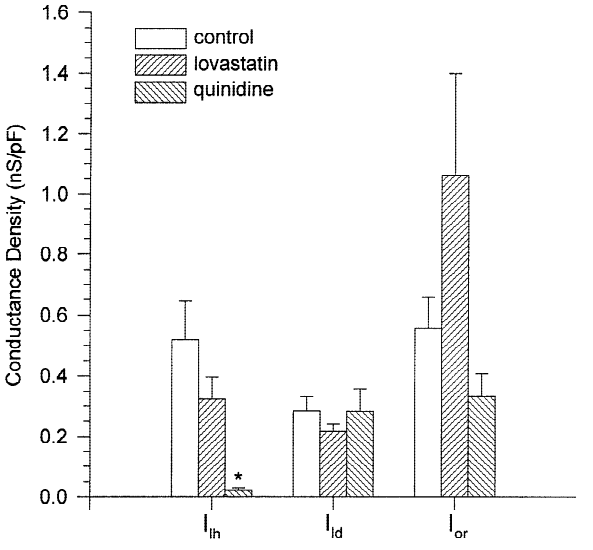

Fig. 10. I_{lh} increases during G1 phase. Current-voltage data were collected from MCF-7 cells arrested in G1 phase by lovastatin ($n = 20$) or quinidine ($n = 13$). Arrest by quinidine significantly decreased I_{lh} alone (asterisk), whereas arrest by lovastatin did not affect any currents.

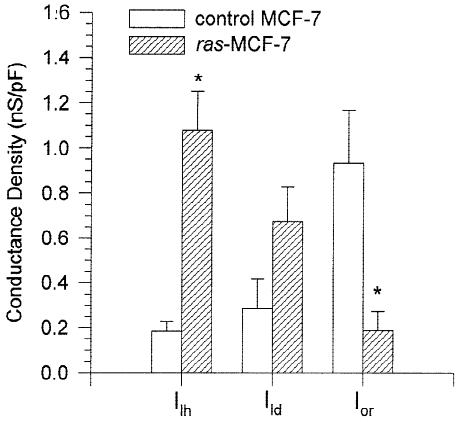

Fig. 11. I_{lh} is larger in *ras*-transformed MCF-7 cells. Current-voltage data were collected from unsynchronized control MCF-7 cells and *ras*-transformed MCF-7 cells. Significant differences in the current densities of *ras*-transformed cells compared to control values are marked by asterisks.

MCF-7 cells, and the shorter transit time probably results from changes in specific cell cycle regulatory signals, such as the observed increase in cyclin D1, a G1 cyclin, and *c-myc* mRNA (J. Strobl, *unpublished data*). We predicted that *ras*-transformed cells are also more hyperpolarized, which might facilitate their passage through G1 phase. We tested this prediction by comparing I_{lh}, I_{ld} and I_{or} in control versus *ras*-transformed cells. I_{lh} was significantly larger in *ras*-transformed cells (Fig. 11). The increase in I_{lh} did not appear to involve expression of a new type of current, because there was no difference in the fractional block of I_{lh} in control and *ras*-transformed cells by 90 μM quinidine (*data not shown*). Cells transformed by *ras* were also less sensitive to arrest by quinidine, the K_i for quinidine was increased 2.8 fold in *ras*-transformed cells (J. Strobl, *unpublished data*). I_{or} was also significantly smaller in *ras*-transformed cells (Fig. 11).

Discussion

I_{LH} is the Target of K Channel Drugs that Arrest the Cell Cycle in G1 Phase

We identified three currents in the macroscopic current-voltage relationships of MCF-7 cells. Among these currents, only the linear hyperpolarized current, I_{lh}, exhibited the properties expected for an ion current that might regulate the progression of MCF-7 cells through early G1 phase. These properties include its sensitivity to agents that arrest the cell cycle, ion selectivity and cell cycle-specific activity. The most prominent feature of I_{lh} was its nearly complete inhibition by millimolar cytosolic ATP, and this warrants the classification of I_{lh} as an ATP-sensitive K current (K_{ATP}). This conclusion is consistent with the ability of antagonists of K_{ATP} currents, but not voltage-gated or Ca-activated currents, to arrest the cell cycle of MCF-7 cells in early G1 phase (Woodfork et al., 1995). However, the position of I_{lh} among the different classes of K_{ATP} currents is unclear. The low potency and very high Hill coefficients of inhibition by glibenclamide and linogliride distinguish I_{lh} from all previously reported K_{ATP} currents, although K_{ATP} currents with low sensitivity to glibenclamide have been reported (reviewed in Gopalakrishnan et al., 1993). We speculate that I_{lh} might be produced by the association of a K channel with a unique sulfonylurea receptor whose ligand-binding properties are different from the SUR or SUR2 subtypes (Inagaki et al., 1996; Ashcroft & Gribble, 1998), and this association might confer the lower sensitivity to glibenclamide and linogliride. Furthermore, although virtually all of I_{lh} could be inhibited by ATP, indicating that it is comprised entirely of K_{ATP} currents, we observed both Ca-independent and Ca-dependent components of I_{lh}, which might be evidence that two types of K_{ATP} currents are present. We have identified an 8 pS K channel in MCF-7 cells that might produce the conductance underlying I_{lh} (Klimatcheva & Wonderlin, 1995); surprisingly, the properties of this channel resemble most closely those of a small-conductance K_{ATP} channel previously identified in the mitochondrial inner membrane (Inoue et al., 1991).

We recently reported that MCF-7 cells arrested in early G1 phase by quinidine could be released from the arrest by treatment with the K^+ ionophore valinomycin, in the continued presence of quinidine (Wang et al., 1998). The ability of valinomycin to overcome the arrest by quinidine demonstrated that inhibition of a K^+ current

was the mechanism responsible for the arrest of the cell cycle by quinidine, and we now conclude that I_{lh} is the K^+ current inhibited by quinidine. We have not yet tested the ability of valinomycin to overcome the arrest by glibenclamide or linogliride. The selectivity of glibenclamide for K_{ATP} currents at the high concentrations required to inhibit I_{lh} might be questionable, because the inhibition of voltage-gated K^+ currents and Cl^- currents at similar concentrations of glibenclamide has been reported (e.g., Tominaga et al., 1995; Vandorpe et al., 1995). However, we can rule out Cl^- currents as the site of action of glibenclamide in MCF-7 cells because the small Cl^- current revealed by introduction of a large Cl^- gradient was not inhibited by glibenclamide. The functional importance of this Cl^- current is not obvious because the membrane potential of MCF-7 cells is not sensitive to changes in the extracellular Cl^- concentration (Wonderlin et al., 1995), and MCF-7 cells do not volume regulate (Altenberg et al., 1994), a common role of some Cl channels. Finally, a TEA-sensitive, outwardly rectifying current, I_{or}, was observed which displayed properties that were opposite from those expected for a current involved in regulating progression through G1 phase. A similar voltage-dependent current has been described in T47D human breast cancer cells (Gallagher et al., 1996), although the reversal potential of its tail currents was more hyperpolarized than the reversal potential for I_{or}. The voltage-dependent activation of I_{or} might function to keep the membrane potential more hyperpolarized than 0 mV, a limit that is evident as a sharp boundary near 0 mV in the distribution of membrane potentials in MCF-7 cells (Fig. 1 in Wonderlin et al., 1995).

The inhibition of I_{lh} by glibenclamide and linogliride was an extraordinarily steep function of drug concentration, especially compared to the inhibition of I_{lh} by quinidine. We previously observed similar, steep relationships for the inhibition of proliferation by glibenclamide and linogliride, but not quinidine (Woodfork et al., 1995). The steepness of the concentration-dependent inhibition might provide further support for the presence of an unusual SUR in MCF-7 cells. We have proposed that the ratio of concentrations at which the cell cycle is arrested by 50% and the K current is inhibited by 50% should be the same for all K channel blocking agents that arrest the cell cycle by selectively inhibiting K currents (Wonderlin & Strobl, 1996), but the incomplete inhibition of I_{lh} by glibenclamide and linogliride prevents us from making this direct comparison. It is clear, however, that there is not a simple relationship among these drugs between the fractional block of I_{lh} and the degree of inhibition of proliferation.

Significance of I_{LH} for Regulating Progression Through G1 Phase

We previously reported that MCF-7 cells in S phase were hyperpolarized by 15–30 mV relative to MCF-7 cells arrested in early G1 phase, and this hyperpolarization was associated with an increase in the relative permeability of the plasma membrane to K^+ (Wonderlin et al., 1995). This increase in the relative permeability to K^+ can be accounted for by the large increase in I_{lh} during progression through early G1 to middle G1 phase, as indicated by the relative sizes of I_{lh} in cells arrested by quinidine and lovastatin, respectively. Furthermore, we conclude that the quinidine-sensitive I_{lh} is the primary, if not the only, physiological mechanism that hyperpolarizes the membrane potential of MCF-7 cells during progression through G1 phase, because the application of quinidine depolarizes all MCF-7 cells to approximately −10 mV (Wang et al., 1998), the membrane potential of cells arrested in early G1 phase (Wonderlin et al., 1995).

The present study provides valuable insight into mechanisms that might coordinate the activity of I_{lh} with other cell cycle signals. We now have direct evidence that the channels which generate I_{lh} can be acutely activated by a fall in the cytosolic ATP concentration or a rise in the cytosolic Ca^{2+} activity, providing rapid, short-term regulation of I_{lh}. On the other hand, the increase in I_{lh} during G1 phase, as revealed by differences in quinidine- *vs.* lovastatin-arrested cells, cannot be accounted for solely by parallel changes in the cytosolic concentrations of Ca^{2+}, ATP or any other freely diffusible cytosolic constituent, because we observed the increase in I_{lh} using ruptured-patch, whole-cell recordings in which the cytosol was dialyzed with the same intracellular solution. Therefore, these channels must also be activated by processes that produce more stable, long-term activation of K_{ATP} channels, such as increased phosphatidylinositol in the cytoplasmic leaflet of the plasma membrane (Shyng & Nichols, 1998; Baukrowitz et al., 1998), protein phosphorylation (e.g., Light et al., 1996), or the expression of additional channels. Although dialysis of the cytosol using the ruptured-patch recording technique provides valuable insight into the mechanisms of activation and regulation of the currents, it will be important in future experiments to examine these currents using a perforated patch recording technique, which will preserve the normal intracellular milieu, thereby providing a more physiologically relevant measure of the activity of the currents at different stages of the cell cycle.

Hyperpolarization by 10–25 mV during progression from early G1 phase to S phase has been observed in rapidly proliferating cells other than MCF-7 cells (Boonstra et al., 1981; Sachs, Stambrook & Ebert, 1974), and it seems plausible that this hyperpolarization is necessary to provide a sufficient electrochemical gradient for the Na-dependent uptake of substrates, such as amino acids, glucose and nucleotides, required for the G1 buildup (Villereal & Cook 1977; Gomez-Angelats et al., 1996). Hyperpolarization might also play a critical role in producing Ca^{2+} signals required for passage through checkpoints in early G1 phase and at the G1/S border (Pittet et

al., 1990; Gelfand, Cheung & Grinstein, 1984; Nilius & Droogmans, 1994). MCF-7 cells can be arrested in G0/G1 by W-13, a calmodulin antagonist (Strobl & Peterson, 1992), which is consistent with a requirement for a Ca signal during their passage through G1 phase. In nonexcitable cells, Ca^{2+} signals are commonly produced by hyperpolarization of the membrane potential, which increases the driving force for the entry of Ca^{2+} through unspecified leak pathways (Nilius, Schwarz & Droogmans, 1993). Nonselective cation channels might function as a pathway for Ca^{2+} entry during G1 progression. Such channels were observed in Balb/c 3T3 cells, in which overexpression of the channels accelerated passage through G1 phase (Kanzaki et al., 1995). I_{ld} included a gadolinium-sensitive component that is probably a nonselective cation current. To the extent that a Ca-permeable, nonselective cation current contributes to I_{ld}, I_{ld} might provide a pathway for the entry of Ca^{2+}. A simple model linking I_{lh} and I_{ld} includes a hyperpolarization of the membrane potential produced by activation of I_{lh} stimulating the entry of Ca^{2+} via I_{ld}, which can then further activate I_{lh}, sustaining the entry of Ca^{2+}. This regenerative model of Ca influx involving interplay between Ca-activated K currents and Ca^{2+} leak pathways has been demonstrated by Nilius and coworkers in melanoma cells (Nilius et al., 1993). Further investigation will be required to test in MCF-7 cells the hypothesis that hyperpolarization is required to produce an obligatory Ca signal during passage through G1 phase.

Finally, if progression through a cell cycle control point requires the activation of K channels and hyperpolarization of the membrane potential beyond a threshold value, then the overexpression or inappropriate activation of K channels would decrease the fraction of channels that need to be activated to reach threshold and pass through the checkpoint, and this might lead to a loss of control at that checkpoint and decrease the potency of K channel blockers that arrest at the checkpoint (Wonderlin & Strobl, 1996). In the present study, we compared I_{lh} in control MCF-7 cells *vs.* MCF-7 cells that overexpress the *ras* oncogene product and display a shorter G1 transit time. We observed that I_{lh} was significantly larger in the *ras*-transformed cells, and we speculate that a diminished regulation of progression through an I_{lh}-dependent checkpoint in early G1 phase might contribute to the more rapid progression of *ras*-transformed cells through G1 phase. The decreased sensitivity of *ras*-transformed MCF-7 cells to arrest by quinidine supports a threshold model in which the activation of I_{lh} is required for passage through a checkpoint in G1 phase (Wonderlin & Strobl, 1996).

The authors would like to thank Dr. Jeannine Strobl for providing unpublished data and Drs. Robert French and Peter Light for their comments on this manuscript. This research was supported by a grant to W.F.W. from the CAMC Foundation L. Newton and Katharine S. Thomas Memorial Fund.

References

Altenberg, G.A., Deitmer, J.W., Glass, D.C., Reuss, L. 1994. P-glycoprotein-associated Cl^- currents are activated by cell swelling but do not contribute to cell volume regulation. *Cancer Res.* **54:**618–622

Ashcroft, F.M., Gribble, F.M. 1998. Correlating structure and function in ATP-sensitive K^+ channels. *TINS* **21:**288–294

Barry, P.H., Lynch, J.W. 1991. Liquid junction potential and small cell effects in patch-clamp analysis. *J. Membrane Biol.* **121:**101–117

Baukrowitz, T., Schulte, U., Oliver, D., Herlitze, S., Krauter, T., Tucker, S.J., Ruppersberg, J.P., Fakler, B. 1998. PIP_2 and PIP as determinants for ATP inhibition of K_{ATP} channels. *Science* **282:**1141–1144

Boonstra, G., Mummery, C.L., Tertoolen, L.G.J., van der Saag, P.T., DeLaat, S.W. 1981. Cation transport and growth regulation in neuroblastoma cells. Modulation of K^+ transport and electrical membrane properties during the cell cycle. *J. Cell Physiol.* **107:**75–83

Edwards, G., Weston, A.H. 1993. The pharmacology of ATP-sensitive potassium channels. *Annu. Rev. Pharmacol. Toxicol.* **33:**597–637

Freedman, B.D., Price, M.A., Deutsch, C.J. 1992. Evidence for voltage modulation of IL-2 production in mitogen-stimulated human peripheral blood lymphocytes. *J. Immunol.* **149:**3784–3794

Gallagher, J.D., Fay, M.J., North, W.G., McCann, F.V. 1996. Ionic signals in T47D human breast cancer cells. *Cell. Signal.* **8:**279–284

Gelfand, E.W., Cheung, R.K., Grinstein, S. 1984. Role of membrane potential in the regulation of lectin-induced calcium uptake. *J. Cell. Phys.* **121:**533–539

Gomez-Angelats, M., Santo, B., Mercader, J., Ferrer-Martinez, A., Felipe, A., Casado, J., Pastor-Anglada, M. 1996. Hormonal regulation of concentrative nucleoside transport in liver parenchymal cells. *Biochem. J.* **313:**915–920

Gopalakrishnan, M., Janis, R.A., Triggle, D. 1993. ATP-sensitive K^+ channels: pharmacologic properties, regulation, and therapeutic potential. *Drug Develop. Res.* **28:**95–127

Harvey, R.D., Clark, C.D., Hume, J.R. 1990. Chloride current in mammalian cardiac myocytes: novel mechanism for autonomic regulation of action potential duration and resting membrane potential. *J. Gen. Physiol.* **95:**1077–1102

Inagaki, N., Gonoi, T., Clement IV, J.P., Namba, N., Inazawa, J., Gonzalez, G., Aguilar-Bryan, L., Seino, S., Bryan, J. 1995. Reconstitution of I_{KATP}: An inward rectifier subunit plus the sulfonylurea receptor. *Science* **270:**1166–1170

Inoue, I., Nagase, H., Kishi, K., Higuti, T. 1991. ATP-sensitive K^+ channel in the mitochondrial inner membrane. *Nature* **352:**244–247

Kanzaki, M., Shibata, H., Mogami, H., Kojima, I. 1995. Expression of calcium-permeable cation channel CD20 accelerates progression through the G1 phase in Balb/c 3T3 cells. *J. Biol. Chem.* **270:**13099–13104

Keyomarsi, K., Sandoval, L., Band, V., Pardee, A.B. 1991. Synchronization of tumor and normal cells from G1 to multiple cell cycles by lovastatin. *Cancer Research* **51:**3602–3609

Klimatcheva, E., Wonderlin, W.F. 1996. A putative K channel (K_{ATP}) regulator of G1 progression in MCF-7 human breast cancer cells. *Biophys. J.* **70:***A*397 (*Abstr.*)

Light, P.E., Sabir, A.A., Allen, B.G., Walsh, M.P., French, R.J. 1996. Protein kinase C-induced changes in the stoichiometry of ATP binding activate cardiac ATP-sensitive K^+ channels. *Circ Res.* **79:**399–406

Lin, C.S., Boltz, R.C., Balek, J.T., Nguyen, M., Talento, A., Fischer, P.A., Springer, M.S., Sigal, N.H., Slaughter, R.S., Garcia, M.L., Kaczorowski, G.J., Koo, G.C. 1993. Voltage-gated potassium channels regulate calcium-dependent pathways involved in human T lymphocyte activation. *J. Exp. Med.* **177:**637–645

Melkoumian, Z., Wang, S., Strobl, J.S. 1997. Effect of the potassium

channel blocker quinidine on estrogen-stimulated cell cycle progression and c-*myc* mRNA levels in MCF-7 human breast cancer cells. *Mol. Biol. Cell* **8:**97

Nilius, B., Droogmans, G. 1994. A role for K^+ channels in cell proliferation. *News Physiol. Sci.* **9:**105–110

Nilius, B., Schwarz, G., Droogmans, G. 1993. Control of intracellular calcium by membrane potential in human melanoma cells. *Am. J. Physiol.* **265:**C1501–C1510

Pittet, D., Di Virgilio, F., Pozzan, T., Monod, A., Lew, D.P. 1990. Correlation between plasma membrane potential and second messenger generation in the promyelocytic cell line HL-60. *J. Biol. Chem.* **265:**14256–14263

Price, M., Lee, S.C., Deutsch, C. 1989. Charybdotoxin inhibits proliferation and interleukin 2 production in human peripheral blood lymphocytes. *Proc. Natl. Acad. Sci. USA* **86:**10171–10175

Sachs, H.G., Stambrook, P.J., Ebert, J.D. 1974. Changes in membrane potential during the cell cycle. *Expt. Cell Res.* **83:**362–366

Sheppard, D.N., Welsh, M.J. 1992. Effect of ATP-sensitive K^+ channel regulators on cystic fibrosis transmembrane conductance regulator chloride currents. *J. Gen. Physiol.* **100:**573–591

Shyng, S.-L., Nichols, C.G. 1998. Membrane phospholipid control of nucleotide sensitivity of K_{ATP} channels. *Science* **282:**1138–1141

Strobl, J.S., Peterson, V.A. 1992. Tamoxifen-resistant human breast cancer cell growth: Inhibition by thioridazine, pimozide and the calmodulin antagonist, W-13. *J. Pharmacol. Exp. Ther.* **263:**186–193

Suzuki, K., Petersen, O.H. 1988. Patch-clamp study of single-channel and whole-cell K^+ currents in guinea pig pancreatic acinar cells. *Am. J. Physiol.* **255:**G275–G285

Tominaga, M., Horie, M., Sasayama, S., Okada, Y. 1995. Glibenclamide, an ATP-sensitive K^+ channel blocker, inhibits cardiac cAMP-activated Cl^- conductance. *Circ. Res.* **77:**417–423

Vandorpe, D., Kizer, N., Ciampollilo, F., Moyer, B., Karlson, K., Guggino, W.B., Stanton, B.A. 1995. CFTR mediates electrogenic chloride secretion in mouse inner medullary collecting duct (mIMCD-K2) cells. *Am. J. Physiol.* **269:**C683–C689

Villereal, M.L., Cook, J.S. 1977. Role of the membrane potential in serum-stimulated uptake of amino acids in a diploid human fibroblast. *J. Supramol. Struct.* **6:**179–189

Wang, S., Melkoumian, Z., Woodfork, K.A., Cather, C., Davidson, A.G., Wonderlin, W.F., Stobl, J.S. 1998. Evidence for an early G1 ionic event necessary for cell cycle progression and survival in the MCF-7 human breast carcinoma cell line. *J. Cell. Physiol.* **176:**456–464

Wegman, E.A., Young, J.A., Cook, D.I. 1991. A 23-pS Ca^{2+}-activated K^+ channel in MCF-7 human breast carcinoma cells: an apparent correlation of channel incidence with the rate of cell proliferation. *Pfluegers Arch.* **417:**562–570

Welsh, M.J. 1984. Anthracene-9-carboxylic acid inhibits an apical membrane chloride conductance in canine tracheal epithelium. *J. Membrane Biol.* **78:**61–71

Wonderlin, W.F., Strobl, J.S. 1996. Potassium channels, proliferation and G1 progression. *J. Membrane Biol.* **154:**91–107

Wonderlin, W.F., Woodfork, K.A., Strobl, J.S. 1995. Changes in membrane potential during the progression of MCF-7 human mammary tumor cells through the cell cycle. *J. Cell Physiol.* **165:**177–185

Woodfork, K.A., Wonderlin, W.F., Strobl, J.S. 1995. Inhibition of ATP-sensitive potassium channels causes reversible cell-cycle arrest of human breast cancer in tissue culture. *J. Cell Physiol.* **162:**163–171

Zhou, H., Tate, S.S., Palmer, L.G. 1994. Primary structure and functional properties of an epithelial K channel. *Am. J. Physiol.* **266:**C809–C824